Università degli Studi di Padova

DIPARTIMENTO DI FISICA E ASTRONOMIA

Corso di Laurea in Fisica

Precession of perihelion of a planetesimal perturbed by a circumstellar disk

Laureando:

Alex Fontana

Matricola 1051537

Relatore:

Prof. Francesco Marzari

Anno Accademico 2014–2015

Contents

Introduction **6**

1 Disk's models **7**
1.1 Binney and Tremaine's model 8
1.1.1 Potential 8
1.1.2 Force 9
1.1.3 Precession rate 10
1.2 Ward's model 10
1.2.1 Potential 10
1.2.2 Force 11
1.2.3 Precession rate 11
1.3 Comparison 11

2 Power-law index $p = 1$ **13**
2.1 Mestel's disk 13
2.1.1 Force 13
2.1.2 Precession rate 14
2.2 Comparison and conclusions 15
2.2.1 Comparison between the models 15
2.2.2 Comparison with a simulation 16

3 Power-law index $p = 3/2$ **19**
3.1 Force 19
3.1.1 Precession rate 20
3.2 Comparison and conclusions 20
3.2.1 Comparison between the models 20
3.2.2 Comparison with a simulation 21

Introduction

Nowadays it is well known that our Solar System was formed after a long time by a dust disk , but in recent years this knowledge has been put to test because of the discovery of extrasolar planets.
One of the many question that scientists are trying to solve is why planets are where they are. Their distance from the system's centre is based on their formation process, which strongly depends on the protoplanetary disk they were born in.
The studies in particular have observed the presence of objects that orbit around binaries, but if wide-separated binaries can be explained, problems arise in the early stages of small separation cases. In this situation the presence of the second star, as Rafikov [7] suggest, leads to a rapid secular evolution, driving planetesimal eccentrities far above the level at which are not destroyed in mutual collisions, so now we would not see any planet.
On the other hand the interactions between a protoplanetary disk and the planetesimals can lead to an apsidal alignment of their orbits, resulting in smaller collision velocities and enabling growth. The combination of this factors leads to the collisional barrier problem, because it results in the fact that inside a certain radius planetesimals can not agglomerate and planets can not exist. The question now is obviously how can we predict that distance from the system center, explaining experimental data.
The solution is deeply related to protoplanetary disks's structure and their interaction with the planetesimal. In Tamayo's *Dynamical stability of imaged planetary systems in formation: application to HL TAU* [9] it is shown that even if we could explain the presence of the planets, it would be really difficult to understand their resonances due to the disk's presence. They are very important to the system's dynamics, because they sometimes provide great stability while in other cases they are destabilizing.
Their locations are usually accurately determined by simple period ratios, however this is only true when the pericenter precession rates are slow compared to orbital rates. This can be assumed if the non-keplerian forces are small perturbations, but for a young system the disk gravity can alterate

this situation, inducing a strong pericenter precession rate and a shift of the location of the resonances.
We see now why is it important to understand the interactions between the disk and the planets, and in particular the disk's induced absidal precession. In this thesis we are studying the disk models that lead to calculate the precession, starting from a surface density function $\Sigma(r) \propto r^{-p}$. The central models analyzed in this paper are taken from Binney and Tremaine's *Galactic Dynamics* [2], used by Tamayo [9], and Ward's *Solar Nebula Dispersal and the Stability of the Planetary System.* They do not assign the p parameter, therefore we can study it in different cases. The main goal is to understand if the results fit with each other and possibly with real cases scenarios *assuming* a certain power-law index for the surface density of the disk.
In the first part we will study the disk-induced potentials $\phi(r)$ from these two models and then confronting them for fixed parameters. Finally we will discuss two simplified models used by Rafikov in [7] and [8]. In the first article he uses Mestel's model [5], which evolves from a $p = 1$ assumption, we will show how to obtain the formulas for the precession rate induced by the interaction forces, then compare it with each of the first two models' results under the same assumptions, in particular the same power-law index. Finally we will compare the predictions and a computer simulation for some reality-based parameters, looking for possible differences.
In the second part we will discuss the results from the second article, where a different index is assumed, $p = 3/2$, which is more used in literature that comes from the Minimum Mass Solar Nebula, [1]. This model is a simplification of Ward's, so it is compared again with its results and the Binney and Tremaine's ones to be tested against a simulation. The articles discuss different dynamical systems, the main distinction between them is the possible presence of another star, however we are comparing each other excluding this kind of situation.

Chapter 1

Disk's models

The purpose of this chapter is to calculate the precession rate of the perihelion of a planetesimal in a young dust disk. To get to the result we follow always the same procedure that starts from the surface density

$$\Sigma(r) = \Sigma_0 \left(\frac{R_t}{r} \right)^p \tag{1.1}$$

where r is the distance from the centre, R_t a fiducial radius and the p index is to be assigned studying the temperature of the disk. We assume that it scales as $T \propto r^{-q}$, with $p = \frac{3}{2} - q$, as suggested by Rafikov [7].
In all models we are going to see R_t becoming a truncation radius, outside of which we assume that the disk is so attenuated that it can be ignored. This is a very interesting point, because the potential inside this radius is not affected by the matter outside as enunciated by Gauss' theorem, so we are ignoring the effects at $r \approx R_t$.
Σ_0 is a constant, that we determined using the disk mass, from

$$M_D = \int_0^{R_t} 2\pi r \Sigma(r) \tag{1.2}$$

that leads to

$$\Sigma(r) = \frac{M_D(2-p)}{2\pi} \frac{1}{(R_t)^2} \left(\frac{r}{R_t} \right)^p \tag{1.3}$$

We always proceed in the calculations keeping the parameter bounded only by $p < 2$.
At this point the models differ on how to express the potential $\phi(r)$ and then the force F_D exercised by the disk on the planetesimal. We are going to see that separately in the next section. In general, once we obtain that, from Murray and Dermott [6] we have a secular disturbing function for a

planetesimal with semimajor axis a and eccentricity vector $\mathbf{e} = (k, h) = (e * \cos\varpi, e * \sin\varpi)$ that is

$$R = na^2 \times \left[\frac{1}{2}(A + \dot{\varpi})(h^2 + k^2) - Bk\right] \tag{1.4}$$

In this equation we grasp the purpose of this study, the precession frequency due to the disk potential, that is

$$\frac{\dot{\varpi}}{n} = -\left[\frac{F_D}{F_K} + \frac{1}{2}r\frac{\partial F_D/\partial r}{F_K}\right] \tag{1.5}$$

where the disk induced force $F_D = \partial\phi/\partial r$, stands as the keplerian force $F_K = GM_\star/r^2$ and $M_\star$ is the star mass. In addition $n = \sqrt{GM_\star/a^3}$ is the mean motion of the planetesimal and G is the gravitational constant. In this paper we don't discuss the other parts of (1.4), such as the A and B terms, but we notice that the evolution equations for the system strongly depend on $\dot{\varpi}$.
At this point we have to construct the potentials to be put into (1.5). It is important to notice that we are building models that will be predictive in the inner region of the disk, in fact deviations are possible at the inner and outer radius because of various effects that we do not consider in this paper.

1.1 Binney and Tremaine's model

1.1.1 Potential

The idea proposed in Binney and Tremaine [2] is that the majority of the matter in a spheroidal distribution around the star is in the proximity of the mid-plane, so we may build a razor-thin axisymmetric disk. We construct the disk potential by adding the potential of infinitely flattended homoeoids into which we have decomposed it. As we can derive from Gauss' theorem, the gravitational field is discontinuous across a sheet of finite surface density, but the potential is continuous. Consequently, the potential in the equatorial plane differs infinitesimally from the potential just above or below the disk. Therefore we need only to calculate the potential at points that are external to all homoeoids and take the limit $z \to 0$ to find the potential in the plane. Finally we get

$$\phi(r, 0) = 4G \int_0^\infty da \arcsin\left(\frac{2a}{(a + r) + |a - r|}\right) \frac{d}{da} \int_a^{R_t} d\zeta \frac{\zeta\Sigma(\zeta)}{\sqrt{\zeta^2 - a^2}} \tag{1.6}$$

1.1.2 Force

From the last formula we can deduce the force

$$F_D(r) = \frac{\partial\phi(r)}{\partial r} = -\frac{4G}{r}\int_0^r da \frac{a}{\sqrt{r^2-a^2}}\frac{d}{da}\int_a^{R_t} d\zeta \frac{\zeta\Sigma(\zeta)}{\sqrt{\zeta^2-a^2}} \tag{1.7}$$

We have put R_t as a cutoff radius, so it replaces the upper limit in the second integral that otherwise should be ∞. From now on we follow Tamayo's work [9], in particular its Appendix, where he suggests that we should look for a disk-induced force that has a non-keplerian correction from the radial one

$$F_D(r) = -F_0\left(\frac{R_t}{r}\right)^p \tag{1.8}$$

where F_0 is a normalization. This could be the forces expression for an infinite disk.
Now (1.7) yelds

$$F_D(r) = -F_0\left(\frac{R_t}{r}\right)^p [1+\eta(r,p)] \tag{1.9}$$

where we have obtained a radial power-law force with a correction factor η, that is fairly complicated. This is the effect of a non-contribution of the parts outside R_t, which is always greater than zero and can be significative. This reflects the fact that the outer material that would have contributed with a positive force is now missing. We have

$$F_0 = \xi(p)\frac{GM_D}{R_t^2} \tag{1.10}$$

and

$$\xi(p) = (2-p)\frac{\Gamma\left[\frac{2-p}{2}\right]\Gamma\left[\frac{1+p}{2}\right]}{\Gamma\left[\frac{3-p}{2}\right]\Gamma\left[\frac{p}{2}\right]} \tag{1.11}$$

where Γ is the Gamma function,

$$\eta(r,p) = \frac{2-p}{\pi\xi(p)}\left(\frac{R_t}{r}\right)^{1-p}\left[2K\left(\frac{r^2}{R_t^2}\right) - \pi H(p,\frac{r^2}{R_t^2})\right] \tag{1.12}$$

with K the elliptic function of the first kind and H the regularized, generalized hypergeometric function

$$ {}_3H_2\left(\{\frac{1}{2},\frac{1}{2},\frac{p-1}{2}\},\{1,\frac{p+1}{2}\},\left(\frac{r^2}{R_t^2}\right)\right) \tag{1.13} $$

We notice that the correction increases as $r \to R_t$ but even if it is normally small is still significative.

1.1.3 Precession rate

With our force (1.9) we have a simple

$$ \frac{\dot{\varpi}}{n} = -\frac{M_D}{M_\star}\left(1-\frac{p}{2}\right)\xi(p)\left(\frac{R_t}{r}\right)^{p-2}[1+\eta_2(r,p)] \tag{1.14} $$

Tamayo does not give an expression for the $\eta_2(r,p)$, so here we do not report the calculations we have made ourselves, because its expression would be inscrutable.
This function is the fractional correction to the case of an infinite disk. We can immediately notice that in the (1.12) the first term is positive and the second one is negative, so the effect of truncating the disk makes F_D more negative, this increases as one approaches R_t. We can see that dF_D/dr decreases, so the first term becomes more positive and the second one less positive. Therefore we can then say that having a cutoff radius for the disk always enhances the magnitude of $\dot{\varpi}$.
The correction $\eta_2(r,p)$ can be quite large, due to the strong effect on the derivative in (1.12), at the outermost gap it is absolutely not omittable.

1.2 Ward's model

1.2.1 Potential

We now start from Ward [10], which Rafikov refers to in [8]. In this case we construct the potential of an uniform circular ring of radius r with linear density l. In particular in a thin planar disk, assumed stationary and with an axisymmetric surface density $\Sigma(r)$ we can replace $l \to \Sigma(r)\,dr$, and integrate between the boundaries. If the nebular density is assumed to be locally *undisturbed* by the planetesimal's presence, we have

$$\phi(r) = 2\pi G r \Sigma(r) \sum_{k=1}^{+\infty} A_k \Bigg[\frac{(4k+1)}{(2k+2-p)(2k-1+p)} - \left(\frac{1}{2k+2-p}\right)\left(\frac{R_{in}}{r}\right)^{2k+2-p} - \left(\frac{1}{2k-1+p}\right)\left(\frac{r}{R_t}\right)^{2k-1+p} \Bigg] \quad (1.15)$$

where $A_k = [(2k)!/2^{2k}(k!)^2]^2$ and R_{in} is an inner cutoff radius caused by the presence of the star that creates a hole in the disks center. Here we see something that the previous model did not consider, but we expect it to be important only at the inner boundaries.

1.2.2 Force

From (1.15) we have the force

$$F_D = \frac{\partial \phi(r)}{\partial r} = 2\pi G \Sigma(r) \sum_{k=1}^{+\infty} A_k \Bigg[\frac{(1-p)(4k+1)}{(2k+2-p)(2k-1+p)} + \left(\frac{2k+1}{2k+2-p}\right)\left(\frac{R_{in}}{r}\right)^{2k+2-p} - \left(\frac{2k}{2k-1+p}\right)\left(\frac{r}{R_t}\right)^{2k-1+p} \Bigg] \quad (1.16)$$

1.2.3 Precession rate

This time we can not provide a readable form of the precession rate because in the (1.5) the derivation of the force leads to a very complicated expression. It will be shown by some graphs in the next chapters when all parameters are going to be fixed.

1.3 Comparison

We have seen that both disk's models start from quite the same assumptions, but because of the different technique of building the potential they can be very different. We have to assign some parameters to represent $\phi(r)$, and the most important is the power index p. In this paper we focus on the $p = 1$ and $p = 3/2$ cases, so we will draw the potentials for these two values. In fact, these are the most used in literature, especially the latter because it is the one on which Minimum Mass Solar Nebula theory is based. Other costants are

- $R_t = 30\,AU$
- $M_D/M_\star = 0.0463385$ for $p = 1$
- $M_D/M_\star = 0.0145898$ for $p = 3/2$
- $R_{in} = 0.5\,AU$

we notice that one mass has to be lower than the other if we want to have the same R_t and respect the Minimum Mass Solar Nebula density law. Now we can plot both potentials for $p = 1$ and $p = 3/2$ respectively.

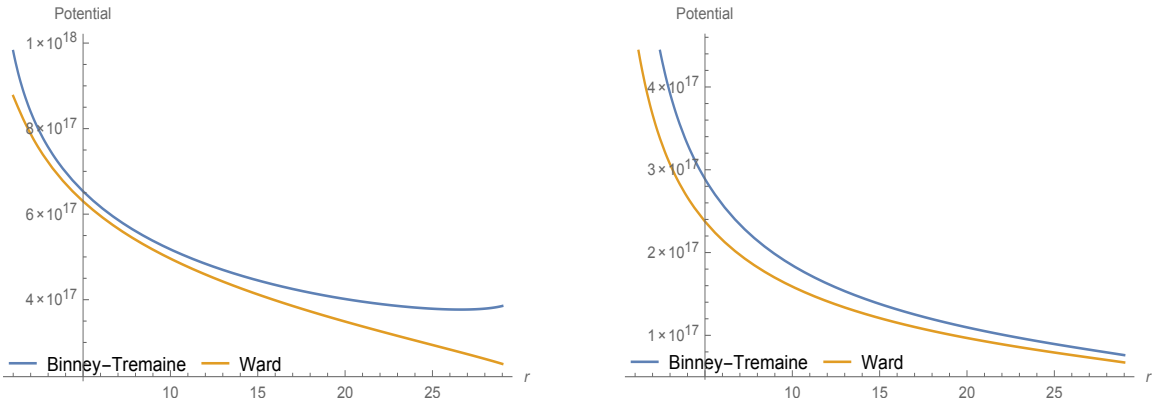

We see that there is a discrepancy, but in the $5 - 15\,AU$ part of the disk there is an approximately constant difference, that should disappear in the force expressions. For the same parameters used before the potential behaviour is now described in the following figure

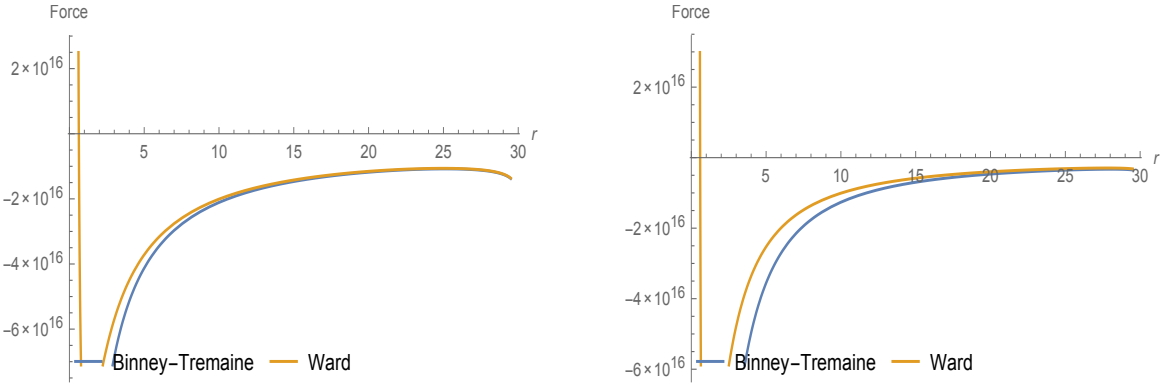

The differences still exist, mostly in the $p = 3/2$ case, and that is an important point because it means that the two disk-building strategies lead to a discordance in the previsions, although small.

Chapter 2

Power-law index $p = 1$

2.1 Mestel's disk

We start from Rafikov's [7] to build the disk, then we use the Mestel's [5] method to obtain the disk induced force and then we derive the precession rate. The structure of the nebula is the same axisymmetric razor-thin disk as before. In the surface density law (1.3) Rafikov assumes $p = 1$ because in the passive disk model described in Chiang and Goldreich [3] we have $p \approx \frac{15}{14}$. This leads to the classical Mestel disk, that corresponds to $R_t \to \infty$. We are going to analyze the motivation of these hypotheses and their consequences.

2.1.1 Force

From Mestel (1963) [3] we extract the disk's potential by integrating circular rings as in the Ward's case. But a different integrals expansion of the density function and the potential itself lead to a similar but not identical formula for the force:

$$\begin{aligned} F_D = & -G\Bigg(\int_0^r \frac{2\pi\zeta\Sigma(r)}{r^2}\,d\zeta \\ & + 2\pi\sum_{k=1}^{+\infty} A_k\left[\frac{2k+1}{r^{2k+2}}\int_0^r \Sigma(r)\zeta^{2k+1}\,d\zeta - \Sigma(r)\right] \\ & + 2\pi\sum_{k=1}^{+\infty} A_k\left[\Sigma(r) - 2kr^{2k-1}\int_r^{R_t}\frac{\Sigma(r)}{\zeta^{2k}}\,d\zeta\right]\Bigg) \end{aligned} \tag{2.1}$$

it is noticeable that this formula resembles the (1.16). The first part is Keplerian, the others are the contributions from the inner and outer mass

of radius r. This is not an important distinction because the non-Keplerian part may be extremely dominant and can not be treated as a perturbation. Mestel tries to simplify the (2.1) and makes this simple assumptions:

$$\begin{aligned} \Sigma(r)r &= const & r &\leq R_t \\ \Sigma(r)r &= 0 & r &> R_t \end{aligned} \tag{2.2}$$

that reduce (2.1) to

$$F_D = -2\pi G\Sigma(r)\left[1 + \sum_{k=1}^{+\infty} A_k \left(\frac{r}{R_t}\right)^{2k}\right] \tag{2.3}$$

Here we eliminated some of the non-Keplerian parts, we proceed further and put $R_t \to \infty$, because we want to concentrate on the inner region of the disk and this leads us to:

$$F_D = -2\pi G\Sigma(r) \tag{2.4}$$

Using (1.3) we have the surface density $\Sigma(r) = \frac{M_D}{2\pi R_t r}$. This could seem a logical contradiction, because it implies that a disk tend to be infinite but has a finite mass. However the hypothesis made in (2.2) keep this real, but we have to remember that this is effective only near the centre of rotation, and also that this is not entirely true because of the omitted effects after (2.4). As we said, the presence of the star cannot be ignored near a certain (although small) radius. We proceed obtaining the simple formula for the drag force from (2.5)

$$F_D = \frac{GM_D}{R_t r} \tag{2.5}$$

This is the final equation for the force by the Mestel's passive classical disk.

2.1.2 Precession rate

We can now use the (1.12) to calculate

$$\frac{\dot{\varpi}}{n} = -\frac{M_D}{M_\star}\frac{r}{R_t} \tag{2.6}$$

Here we see that the precession rate and the radius are in linear dependence.

2.2 Comparison and conclusions

We can now compare the three previous models upon the results they gave, then we are going to run a computer simulation to see if they are consistent.

2.2.1 Comparison between the models

The formulas extracted to calculate the perihelion's precession rate of a planetesimal have deep differences, but to fully appreciate them we have to consider the hypothesis and simplifications. Both methods have introduced a truncation radius that is R_t, to determine the constant in the power law surface density formula. Mestel's theory assumes that this *has* to be proportional to the inverse of the radial distance, $p = 1$, while Binney and Tremaine and Ward keep that value free to be fixed by experimental observations.
Also the truncation radius is sent to infinite in order to have the simple formula of Mestel's force. On the contrary the other methods do not require this hypothesis, in fact for example in the (1.7) we substitute ∞ with R_t in the integration to represent a finite disk.
Now we want to see where the same starting conditions lead us, confronting the precession rates. Mestel's model being more strict forces us to put $p = 1$ in Binney and Tremaine's and Ward cases. If this should lead us to the same formula, it would be clear that the first two models are more complex and give the same results when the hypothesis are near the Mestel's ones. Again, it is possible to show a scrutable expression only for the Binney and Tremaine's precession, Ward's case is going to be shown graphically. In (1.14) we have $\xi(1) = 1$, and the result is:

$$\frac{\dot{\varpi}_{BT}}{n} = -\frac{1}{\pi}\frac{M_D}{M_\star}\frac{r}{R_t}\frac{1}{(1 - r^2/R_t^2)}E\left[\frac{r^2}{R_t^2}\right] \tag{2.7}$$

where $E\left[\frac{r^2}{R_t^2}\right]$ is the elliptic integral of the second kind. Here we notice a very important thing, because if we put $R_t \to \infty$ we have:

$$\frac{\dot{\varpi}_{BT}}{n} = -\frac{1}{2}\frac{M_D}{M_\star}\frac{r}{R_t} \tag{2.8}$$

because $E[0] = \pi/2$. This is Mestel's second simplification, now we compare the Binney and Tremaine's formula with:

$$\frac{\dot{\varpi}_{M}}{n} = -\frac{M_D}{M_\star}\frac{r}{R_t} \tag{2.9}$$

They do not give the same predictions, there is a 50% shift.
This is a very big correction given by Binney and Tremaine, it is nevertheless

very important not to forget the validation limits given by Mestel. We can calculate the precession in this way in a medium - inner region of the disk to avoid the deviations at the center but more importantly at the outer.

2.2.2 Comparison with a simulation

In this paragraph we have to understand which model is more predictive, so we can try and take a real-case disk and run a computer simulation on a hypothetic planetesimal. This is a program named FARGO [4] that computes the Navier-Stokes equations for a disk with the same parameters we have assigned in chapter 1. They are:

- $R_t = 30\,AU$
- $M_D/M_\star = 0.0463385$
- $R_{in} = 0.5\,AU$

We want to calculate a precession for a determined distance from the centre, so we choose $r = 5\,AU$.
We start from confronting the models. We put these data in the (2.7) because if we used (2.9) and tested it with (2.10) we would simply see a difference of a 1/2 factor. This also is fundamental to demonstrate which model is more realistic with no other limit than $p = 1$. Now it is possible to make previsions for the Ward model too. Here are the three results:

$$\frac{\dot{\varpi}_{BT}}{n} = -0.00395 \quad , \frac{\dot{\varpi}_W}{n} = -0.00395 \quad , \frac{\dot{\varpi}_M}{n} = -0.00773 \tag{2.10}$$

We can see that the first value is not exactly half of the third value but it is fairly close. It is also noticeable that Ward's previsions and Binney and Tremaine's precession are the same.
These numbers are in normalized units, but we want to extract the precession rate without dividing for the mean motion, in order to do this we multiply for $\frac{2\pi}{11.2}\left(\frac{5}{r}\right)^{1.5}$. It is the same procedure as using Kepler's Third Law $r^3/T^2 = cost$ where r is the radius of the planetesimal's orbit and T is its period.

$$\dot{\varpi}_{BT} = -0.00222\,yr^{-1}\,, \dot{\varpi}_W = -0.00221\,yr^{-1}\,, \dot{\varpi}_M = -0.00434\,yr^{-1} \tag{2.11}$$

The planetesimal in the computer-simulated disk has:

$$\dot{\varpi}_{calc} = -0.00218\, yr^{-1} \tag{2.12}$$

that is very similar to the first two results.
Other combinations of parameters has been tested, and the aftermaths are almost unanimous: the Mestel's model does not give an accurate prediction of our reality-simulated system, while the others do. Here we present some precession rates at different radius calculated with the three methods and the simulation.

	$\dot{\varpi}_{BT}\,(yr^{-1})$	$\dot{\varpi}_{W}\,(yr^{-1})$	$\dot{\varpi}_{M}\,(yr^{-1})$	$\dot{\varpi}_{calc}\,(yr^{-1})$
5 AU	-0.00222	-0.00221	-0.00434	-0.00218
7 AU	-0.00191	-0.00191	-0.00366	-0.00185
9 AU	-0.00173	-0.00173	-0.00323	-0.00172
11 AU	-0.00163	-0.00163	-0.00292	-0.00165
13 AU	-0.00157	-0.00157	-0.00269	-0.00161
15 AU	-0.00156	-0.00156	-0.00250	-0.00161

We can conclude that Mestel's model is oversimplified and can not be used without introducing a big error. To fully appreciate the differences between these models we can plot the $\dot{\varpi}(r)$.

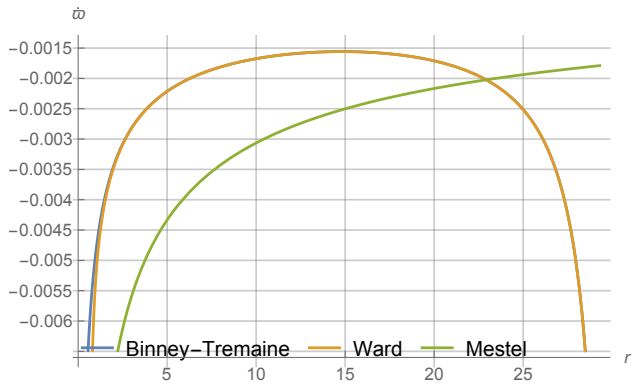

It is clear that between the Mestel model and the others there is a huge divergence. In fact the precession rate for a planetesimal in a Mestel's disk grows until it reaches the cutoff radius, while in the other structure's disk it has a rapid diminution near the center and the outer regions. The simulation cannot produce a graphic of $\dot{\varpi}$ dependent from the radius, but from the previous table we can visualize its trend. It is also interesting to see a section of this curves:

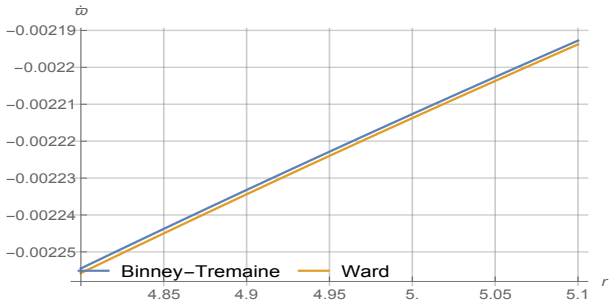

Zoom of the Binney-Tremaine's and Ward's curves

The Binney and Tremaine's and Ward's precessions are very similar, in fact in the first graph we see only two lines because the separation between Ward's and Binney and Tremaine's curves is at always less than 10^{-5} so we can not see any differences through all the way to the outer radius. This is shown in the second figure for a distance near 5 AU and this can be read as a confirmation that the two disk models are almost identical for our purpose. We can summarize the conclusions of this study:

- To calculate the precession of the perihelion of a planetesimal in a disk, having hypothesize a power index $p = 1$, we should avoid the Mestel's formula, even if our object was in the inner part of the disk.
- Between Ward's and Binney and Tremaine's models for the $\dot{\varpi}(r)$ there aren't noticeable differences, even if their potentials had. Therefore either one can be used without problems.
- The computer simulation has proved that these two models are remarkably representative of the reality.

Chapter 3

Power-law index $p = 3/2$

We now present the results for the (1.1) for a different p index from the $p = 1$ suggested by Rafikov (2013) [7], in fact in [8] he uses a $p = 3/2$, similar to the $\Sigma(r)$ slope of the Minimum Mass Solar Nebula. This is a very commonly used index, so there is a hint that induces us not to trust Mestel's model, because it may require a biased assumption.
In these articles Rafikov studies a binary system, where it is very important an inner cutoff radius R_{in} because of the the torque due to the binary that stops the inward flow of matter. We are going to exclude the presence of the second star; anyway, it would only change our model near the inner radius.
The method we present here is a simplification of Ward's potential, the aim is to understand how the precession rate calculated are consistent with Ward's and Binney and Tremaine's.

3.1 Force

We start from (1.16), Rafikov here makes two assumptions, $R_{in} \to 0$ and $R_t \to \infty$, to eliminate the second and third part of (1.16). This can be accepted for a large disk with a very small inner radius, and it is similar to Mestel's second simplification. This results in:

$$F_D = 2\pi G\Sigma(r) \sum_{k=1}^{+\infty} A_k \left[\frac{(1-p)(4k+1)}{(2k+2-p)(2k-1+p)} \right] \tag{3.1}$$

It is clear that the effect is a less complicated and more handy formula. We are going to assign $p = 3/2$ in order to show a general formula first.

3.1.1 Precession rate

We now take the perihelion precession for the (3.1) with (1.5), we obtain:

$$\frac{\dot{\varpi}_R}{n} = -\frac{K_d}{16}\frac{M_D}{M_\star}\left(\frac{r}{R_t}\right)^{1/2} \tag{3.2}$$

where $K_d(p) = \sum_{k=1}^{+\infty} A_k \frac{(4k+1)}{(2k+2-p)(2k-1+p)}$. In the article [8] this is calculated for a binary system, but Ward does not take this as an assumption so we can use this formula for a single star case.
We expect a very close similarity in the center region with Ward's results.

3.2 Comparison and conclusions

It is now possible to compare Binney and Tremaine's formula with Ward's and Rafikov's, then adding a computer simulation.

3.2.1 Comparison between the models

All models start from the same hypothesis, except from the fact that Rafikov greatly simplifies the disk-induced force. We put in each precession rate formulas $p = 3/2$, but in this case the (1.13) does not assume a readable form, we get:

$$\frac{\dot{\varpi}_{BT}}{n} = -\frac{1}{4}\xi(1.5)\frac{M_D}{M_\star}\left(\frac{r}{R_t}\right)^{1/2}[1 + \eta_2(r, 1.5)] \tag{3.3}$$

We have $\xi(1.5) = 1.094$, so if we assume that $\eta_2 \approx 0$, which is quite true far from the outer boundaries, we can write:

$$\frac{\dot{\varpi}_{BT}}{n} \approx -0.2730\frac{M_D}{M_\star}\left(\frac{r}{R_t}\right)^{1/2} \tag{3.4}$$

This is to be compared with Rafikov's (3.2)

$$\frac{\dot{\varpi}_R}{n} \approx -0.2735\frac{M_D}{M_\star}\left(\frac{r}{R_t}\right)^{1/2} \tag{3.5}$$

because $K_D \approx 4,3769$. We see that the formulas lead to almost the same results, as we expected for zones far from the critical regions. We can not report the Ward's precession at this point, but we will show in the next part its value for fixed parameters.

3.2.2 Comparison with a simulation

It is now possible to put to test with the computer-simulated disk these results. Feeding (3.3), (3.5) and also Ward's formula with

- $R_t = 30\,AU$
- $M_D/M_\star = 0.0149858$
- $R_{in} = 0.5\,AU$

we can have our results on a $r = 5\,AU$. This time we put the results directly in yr^{-1}

$$\dot{\varpi}_{BT} = -0.000945\,yr^{-1},\ \dot{\varpi}_W = -0.000947\,yr^{-1},\ \dot{\varpi}_R = -0.000939\,yr^{-1} \tag{3.6}$$

Now the computer simulation calculates

$$\dot{\varpi}_{calc} = -0.00108\,yr^{-1} \tag{3.7}$$

At $5\,AU$ they are all quite similar to each other; here we present some precession rates at different radius calculated with the three methods and the simulation.

	$\dot{\varpi}_{BT}\,(yr^{-1})$	$\dot{\varpi}_W\,(yr^{-1})$	$\dot{\varpi}_R\,(yr^{-1})$	$\dot{\varpi}_{calc}\,(yr^{-1})$
5 AU	-0.000945	-0.000947	-0.000939	-0.00108
7 AU	-0.000681	-0.000681	-0.000663	-0.000747
9 AU	-0.000537	-0.000537	-0.000523	-0.000592
11 AU	-0.000449	-0.000449	-0.000437	-0.000506
13 AU	-0.000391	-0.000392	-0.000381	-0.000448
15 AU	-0.000354	-0.000354	-0.000345	-0.000424

We notice an important thing: Binney and Tremaine's precession rates are almost identical with Wards, but there is a $10 - 15\%$ shift from the simulation. This is not a big difference, but it is significative because it means that our models have a small lack in their prevision power. Again we can plot the $\dot{\varpi}(r)$

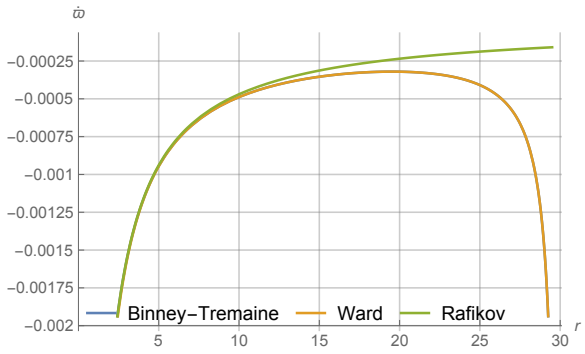

Here we see the same problem of Mestel's model, the planetesimal have an apsidal precession that goes to zero at the external boundaries in Rafikov's approximation. In fact it is shown that the more we go to the outer boundaries, the worse Rafikov's previsions are.

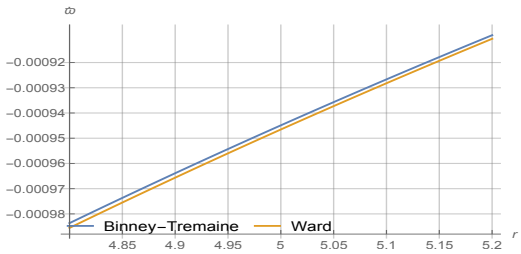

Zoom of the Binney-Tremaine's and Ward's curves

Here we see again the small separation of these two previsions.
We can now summarize the conclusions of this study:

- To calculate the precession of the perihelion of a planetesimal in a disk we hypothesized having a power index $p = 3/2$ we can use all of our three models, if our object is in the inner part of the disk.
- Between Ward's and Binney and Tremaine's models for the $\dot{\varpi}(r)$ there aren't noticeable differences, either one of them can be used without distinction.
- When we try to study a planetesimal near the boundaries, even if the models can differ a lot from reality, the best solution we find is to use the Ward's model for the inner part while for the outer one it is the same to use Binney and Tremaine's or the previous.
- The computer simulation has led us to the important confirmation that all three models give quite a good representation of the reality, even if they present a significative shift. Therefore one approaching the study should keep in mind that for this power index the error could be around $10 - 15\%$.

Bibliography

[1] P. J. Armitage, *Astrophysics of Planet Formation*, Cambridge University Press, (2010) 4-5.

[2] J. Binney, S. Tremaine *Galactic Dynamics*, 2nd Edition, Princeton Series in Astrophysics, Princeton University Press (2008), 96-100.

[3] E. I. Chiang, P. Goldreich, *Spectral energy distributions of T Tauri Stars with passive circumstellar disks*, Astrophisical Journal, 490: 368-376, (1997), 370-371.

[4] F. Masset, *FARGO*, http://fargo.in2p3.fr/.

[5] L. Mestel, *On the galactic law of rotation*, MNRAS.126, 553-575, (1963), 556-559.

[6] C. D. Murray, S. F. Dermott, *Solar System Dynamics*, Cambridge University Press, (1999).

[7] R. R. Rafikov, *Planet formation in small separation binaries: not so secularly exiced by the companion*, Astrophisical Journal Letters 765:L8, (2013).

[8] R. R. Rafikov, *Building Tatooine: suppression of the direct secular excitation in Kepler circumbinary planet formation*, Astrophisical Journal Letters 764:L16, (2013).

[9] D. Tamayo, A. H. M. J. Triaud, K. Menou, H. Rein *Dynamical stability of imaged planetary systems in formation: application to HL Tau*, Astro-Ph EP, (2015), 7-8, 13-15.

[10] W. R. Ward, *Solar Nebula Dispersal and the Stability of the Planetary System*, ICARUS 47, 234-264, (1981), 260-263.